The current issue and full text archive of this journal is available at
www.emeraldinsight.com/0961-5539.htm

Multi-scale thermo-fluid transport in porous media

Emre Sozer and Wei Shyy
Aerospace Engineering Department, University of Michigan, Ann Arbor, Michigan, USA

Received 15 September 2007
Accepted 18 December 2007

Abstract

Purpose – The purpose of this paper is to develop an empiricism free, first principle-based model to simulate fluid flow and heat transfer through porous media.

Design/methodology/approach – Conventional approaches to the problem are reviewed. A multi-scale approach that makes use of the sample simulations at the individual pore levels is employed. The effect of porous structures on the global fluid flow is accounted for via local volume averaged governing equations, while the closure terms are accounted for via averaging flow characteristics around the pores.

Findings – The performance of the model has been tested for an isothermal flow case. Good agreement with experimental data were achieved. Both the permeability and Ergun coefficient are shown to be flow properties as opposed to the empirical approach which typically results in constant values of these parameters independent of the flow conditions. Hence, the present multi-scale approach is more versatile and can account for the possible changes in flow characteristics.

Research limitations/implications – Further validation including non-isothermal cases is necessary. Current scope of the model is limited to incompressible flows. The methodology can accommodate extension to compressible flows.

Originality/value – This paper proposes a method that eliminates the dependence of the numerical porous media simulations on empirical data. Although the model increases the fidelity of the simulations, it is still computationally affordable due to the use of a multi-scale methodology.

Keywords Flow, Fluid dynamics, Porous materials

Paper type Research paper

Nomenclature

A	= cross-sectional area
A_{sf}	= solid-fluid interfacial area
C_E	= Ergun coefficient
δ_{ij}	= Kronecker delta
ε	= porosity
K	= permeability
k_f	= fluid phase thermal conductivity
k_s	= solid phase thermal conductivity
$\dot{m}$	= mass flow rate
μ	= dynamic viscosity
n_i	= surface normal vector
p	= pressure
ρ	= fluid density
Re_D	= Reynolds number based on pore diameter
$Re_{\sqrt{K}}$	= Reynolds number based on permeability
T_{ij}	= stress tensor
T	= temperature
u_D	= filter velocity
u_i	= velocity vector
V_f	= volume of the fluid phase
V	= total volume

This study is supported by the NASA Constellation University Institute Program. The authors have benefited from collaboration with Dr Siddharth Thakur, and Professors Bruce Carroll and Jacob Chung of the University of Florida, Professor Jack Hu and Dr Guosong Lin of the University of Michigan, and Mr Kevin Tucker of NASA Marshall Space Flight Center.

International Journal of Numerical Methods for Heat & Fluid Flow
Vol. 18 No. 7/8, 2008
pp. 883-899

0961-5539
DOI 10.1108/09615530810899006

1. Introduction

Porous materials are often used for the injector face plate of liquid rocket engines. Fuel bleeds through the porous plate to aid in cooling of the injector face by transpiration. In P&W's RL10 engine and Space Shuttle Main Engine (SSME), Rigimesh porous material is used (Sutton, 2003). Rigimesh can qualitatively be classified as a dense, non-uniform, fibrous porous media (Figure 1). In the case of SSME, a 0.25″ thick plate with about 9 percent void space is used. Our ultimate goal in this study is accurate simulation of fluid flow and heat transfer through the Rigimesh material. To achieve this, we need detailed knowledge of the material's internal structure.

Fluid flows and associated heat and mass transfer through such porous media are two-phase phenomena where one of the phases is solid and stationary. To simulate such flows, interaction of fluid and solid phases at the scales as small as individual pores of the material needs to be accounted for. Considering typically wide range of length scales and complex geometries involved in porous media, analysis of each individual pore can be very costly or even impossible. Thus, the modeling efforts in this area dating back to Darcy's (1856) experimental study in 1856 have mostly aimed at empirically correlating the pore level flow effects to the bulk fluid motion. Darcy experimented with gravity driven flow of water through a porous medium of loosely packed, uniform sized particles. He related the pressure gradient to the average fluid velocity, introducing an empirical factor called permeability:

$$-\nabla p = \frac{\mu}{K} u_D \tag{1}$$

The permeability, K with the dimension of length^2 is a measure of fluid flow conductivity of the porous media. The filter velocity, u_D, is defined as:

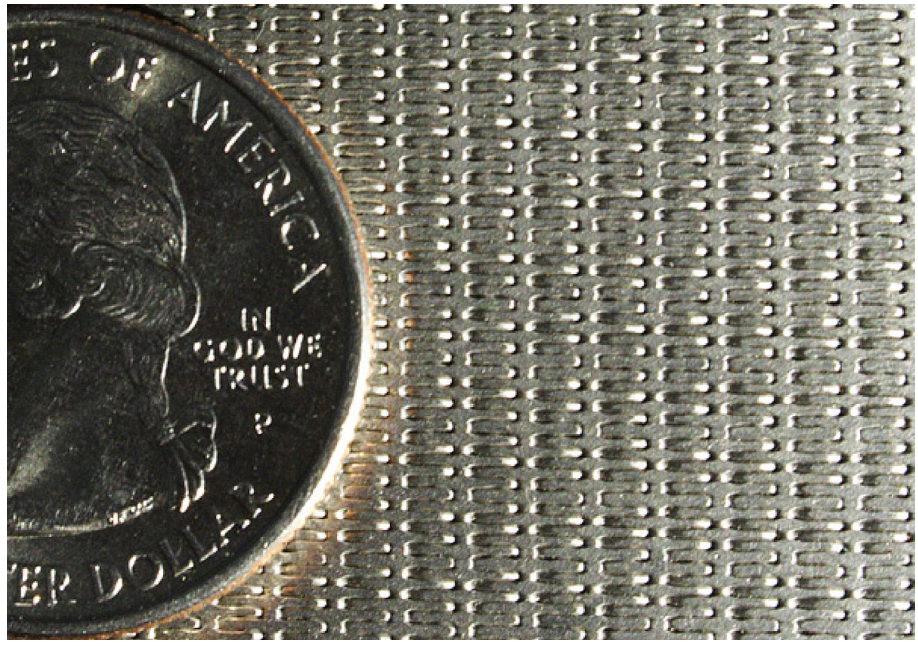

Figure 1.
Surface features of the Rigimesh material used in SSME

$$u_D = \frac{\dot{m}}{\rho A}. \tag{2}$$

Equation (1) is of first order and as such it only allows one condition to be applied at a given boundary. This becomes a problem when the porous matrix is bounded by walls or adjacent to an open flow domain. Typical practice for walls is to apply a slip boundary condition by setting only the velocity component normal to the wall as zero. For the open/porous domain interface, an empirical boundary condition is derived by Beavers and Joseph (1967).

An alternative formulation governing the fluid flow through porous media is suggested by Brinkman (1947, 1948) by adding a viscous diffusion term to the Darcy's law, obtaining a second order equation:

$$-\partial_i p = \frac{\mu}{K} u_{D_i} + \mu' \partial_j^2 u_{D_i}, \tag{3}$$

where μ' is termed as effective viscosity. Lundgren (1972) studies and justifies the Brinkman equation and connects the effective viscosity, μ', to the porosity of the solid matrix. Porosity, ε, is defined as the volume fraction of the void space in a given porous media. Brinkman equation was derived for a dilute arrangement of spheres and thus deemed valid for high porosities, i.e. $\varepsilon > 0.8$ (Rubinstein, 1982). For lower porosity cases, the Darcian contribution dominates and the viscous diffusion term serves the purpose of raising the order of the equation so that the no-slip condition can be applied at bounding walls. Therefore, it is a common practice to set the effective viscosity, μ', equal to the fluid viscosity, μ.

The linear relationship represented by Darcy's law fails when the flow Reynolds number is high enough for inertial effects to become comparable to Darcian effects. Macdonald *et al.* (1979) examines several experimental results and concludes that the inertial flow regime starts roughly when a Reynolds number based on permeability, $Re_{\sqrt{K}} = \rho u_D \sqrt{K}$, is unity. At higher Reynolds numbers, inertial effects become comparable to Darcian effects. A correction for this flow regime is suggested by Forchheimer (1901) and presented in the following form by Ward (1964):

$$-\partial_i p = \frac{\mu}{K} u_{D_i} + \frac{C_E}{\sqrt{K}} \rho |u_{D_i}| u_{D_i}, \tag{4}$$

where C_E is called the Ergun (1952) coefficient. It is also widely used as C_F which stands for Forchheimer coefficient.

Equation (4) involves two parameters; permeability, K, and Ergun coefficient, C_E, which need to be found experimentally for a specific type of porous media. Various methods have been suggested to relate these parameters to the geometrical properties of the porous material such as the porosity and a length scale. Dullien (1979) suggests modeling the porous media as a network of conduits. Using the Hagen-Poiseuille solution, Darcy's law (equation (1)), and total pressure drop, he relates the permeability to porosity and the conduit volumes and diameters. In a similar approach, porous media is modeled as periodic arrangements of cylinders (Sparrow and Loeffler, 1959; Happel and Brenner, 1986) or spheres (Happel and Brenner, 1986) so that the creeping flow solution is benefited in relating the permeability to the porosity, particle diameters and inter-particle gaps. Dullien (1979) also suggests a widely used permeability model

based on the Carman-Kozeny hydraulic radius theory (Carman, 1937). In this model, permeability is related to the porosity, hydraulic radius and Kozeny constant which depends on the pore shape. For the Ergun coefficient, Ward (1964) suggests a universal constant value of 0.55. These heuristic approaches summarized here are mostly limited in range of porous media types and suffer from a common underlying assumption of permeability and Ergun coefficient being pure geometric parameters. We will show later that this is in fact not the case. Detailed summary on this kind of approaches can be found in Dullien (1979), Kaviany (1991) and Nield and Bejan (1992).

The modeling approaches we have mentioned so far have been empirical, semi-empirical or *ad hoc*. A more fundamental approach has been developed by Slattery (1969, 1981) and Whitaker (1969, 1996) by averaging the governing equations over local volume elements that contain both fluid and solid phases. Although this will reduce the complexity of the problem, the information lost by filtering the fine scale flow structures will cause an unclosed set of governing equations. Whitaker (1996) and Nozad *et al.* (1985) also offer closure methodologies for the averaged momentum and energy equations, respectively. Local volume averaging method has gained widespread popularity in modeling fluid flow and heat transfer through porous media. Conventionally, the resulting closure terms in the averaged momentum equations are heuristically linked (Vafai and Tien, 1981) to the relations proposed by Darcy and Ergun which require empirical determination of the parameters K and C_E.

Cheng and Minkowycz (1977), on the other hand, developed another rigorous formulation by introducing a similarity solution for Darcian free convection along a boundary layer developing in a fluid saturated porous medium adjacent to a heated vertical wall. This approach is later extended to combined free and forced convection about inclined walls (Cheng, 1977), non-Darcian (inertial) regime (Bejan and Poulikakos, 1984), mixed convection-conduction problems (Liu *et al.*, 1986) and many other boundary layer type flows. An inclusive coverage of these methods can be found in Nield and Bejan (1992).

To develop non-empirical predictive capabilities for porous media problems, we follow a first principle based, multi-scale strategy. In our approach, the effect of porous structure on the global fluid flow is accounted for via local volume averaged governing equations. The resulting set of transport equations contains closure terms representing the statistical flow characteristics around the pores. Most porous media can be thought of as a matrix of repeating pore patterns. So, the closure terms can be deduced beforehand by direct computation of the fluid flow in individual, representative pore samples for varying flow speeds. Thus, we can avoid the excessive computational cost of direct simulation yet we can produce accurate numerical predictions completely free of empiricism.

In this paper, we first describe the issues related to the characterization of the Rigimesh material. Then, we review derivation of local volume averaged governing equations as well as closure methodologies. The developed model is incorporated into Navier-Stokes solvers (Thakur *et al.*, 2002; Kamakoti *et al.*, 2006; Shyy, 1994) and assessed using a recent experiment by Tully *et al.* (2005) motivated by the liquid rocket engine applications.

2. Rigimesh characterization

Rigimesh is a porous material with sintered multiple layers of stainless steel woven-wire-meshes. Bonding of fibers at each contact point due to the sintering

process provides rigidity and thus allows finer fiber diameters to be employed. Finer fiber diameters in effect mean more surface area for a given volume or porosity. These properties make Rigimesh an appropriate fit for the applications that demand high-cooling efficiency and rigidity. One such area is the injector face plate of liquid propellant rocket engines.

In order to develop high fidelity models for the simulation of flow and heat transfer through the Rigimesh media, precise understanding of the inner topology as well as the inner dimensions is essential.

In order to characterize the Rigimesh structure, a plate sample of 5.8 mm thickness is examined. Although the surface was hinting a woven structure, examining the cross-section was needed to identify the orientation of layers. In order to get a clean cross-sectional view of the material, a plate sample is fractured by bending. Although the bending process caused elongation and distortion of the fibers, the cross-section view obtained (Figure 2) gave valuable clues about the inner topology.

A Rigimesh specimen was analyzed using CT scan. Unfortunately, the CT images did not have enough resolution to offer more information about the material. The surface properties of the Rigimesh were also examined by the contact profilometer measurement technique. A sensitive needle is traversed along the surface of the Rigimesh plate while maintaining contact. Position of the needle tip is recorded every 0.5 μm for a 10 mm span. Lin and Hu (2007) have conducted the measurements. Their results show that the average distance between the peaks is 0.42 mm which is a measure of distance between fiber axes on the surface. The outcome is shown in Figure 3.

The information obtained thus far about the detailed Rigimesh structure helps to illustrate some aspects of Rigimesh; more efforts are needed to fully characterize the 3D geometric structures.

3. Multi-scale porous media model

3.1 Local volume averaging

In the context of averaging the governing equations, first a sensible scale for an averaging volume needs to be defined. An averaging volume should be sized small enough in order to not filter global flow structures but it should be large enough so as to guarantee containing both fluid and solid phases at all times. Such a volume is

Figure 2.
Rigimesh cross-section after bending fracture

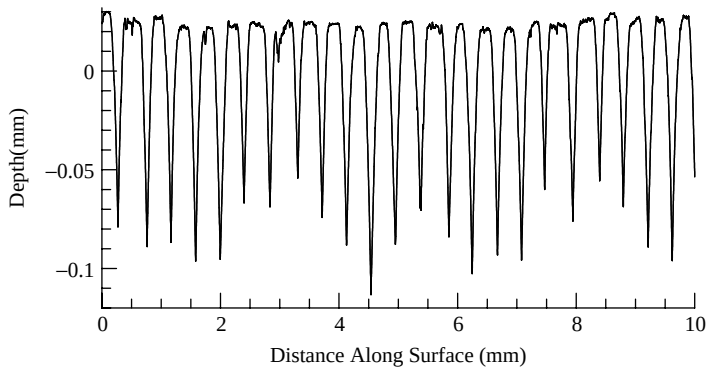

Figure 3.
Rigimesh surface characterization

Source: Lin and Hu (2007)

called as a representative elementary volume (REV) (Figure 4). In our multi-scale methodology, we further require an REV to be a repeated pattern over a portion of the porous media.

The porosity, ε, is defined as the volume fraction of fluid phase in a porous media:

$$\varepsilon = \frac{V_f}{V}. \tag{5}$$

Note that the porosity might be defined locally or globally depending on the scale that the volume fraction is calculated. In this study, however, we will assume that the porosity is uniform over the porous media.

For an arbitrary property ψ defined for the fluid phase, volume averaging can be carried out as follows (Whitaker, 1996):

Intrinsic averaging:

$$\langle \psi \rangle^f = \frac{1}{V_f} \int_{V_f} \psi \mathrm{d}V. \tag{6}$$

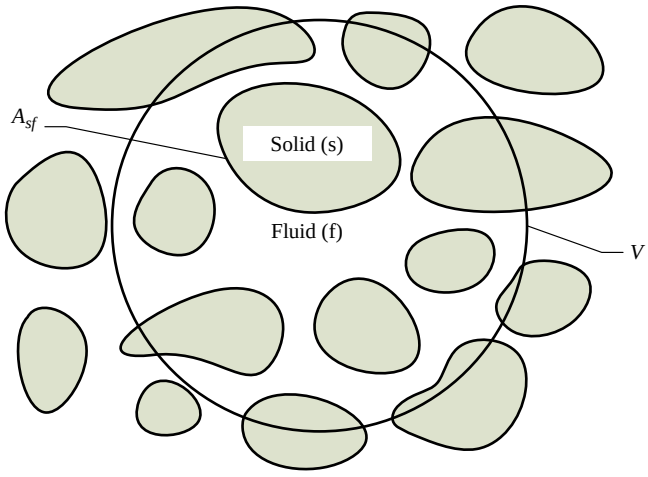

Figure 4.
Schematic of a REV

Superficial averaging:

$$\langle\psi\rangle = \frac{1}{V}\int_{V_f} \psi \mathrm{d}V = \varepsilon\langle\psi\rangle^f. \tag{7}$$

3.2 Averaging of the continuity equation

The local volume averaged continuity equation can be written as:

$$\frac{\partial\langle\rho\rangle}{\partial t} + \langle\partial_i(\rho u_i)\rangle = 0, \tag{8}$$

Note that we want to solve for volume averaged flow quantities. So we need to express the second term in equation (8) in terms of $\langle\rho\rangle$ and $\langle u_i\rangle$. The necessary transformation can be achieved via the volume averaging theorem (Slattery, 1969; Whitaker, 1969):

$$\langle\partial_i\psi\rangle = \partial_i\langle\psi\rangle + \frac{1}{V}\int_{A_{sf}} \psi n_i \mathrm{dA}. \tag{9}$$

Here, n_i is the area normal pointing from the fluid phase towards the solid phase.

Using equation (9), equation (8) becomes:

$$\frac{\partial\langle\rho\rangle}{\partial t} + \partial_i\langle\rho u_i\rangle + \frac{1}{V}\int_{A_{sf}} \rho u_i n_i \mathrm{dA} = 0. \tag{10}$$

Since the fluid will be at rest at the solid-fluid interface due to the no-slip condition, the last term in equation (10) vanishes, and we get:

$$\frac{\partial\langle\rho\rangle}{\partial t} + \partial_i\langle\rho u_i\rangle = 0. \tag{11}$$

For incompressible flows:

$$\partial_i\langle u_i\rangle = 0. \tag{12}$$

Thus, the form of the continuity equation is unchanged by local volume averaging for incompressible flows. In the case of compressible flows, we need to have a special treatment for averaging of the product of the density and the velocity component.

The derivations hereafter assume incompressible flow with constant properties. We further consider that the porosity is constant throughout the porous media. These aspects can be generalized.

3.3 Averaging of the momentum equation

Averaging the momentum equation with no body forces yields:

$$\rho\frac{\partial\langle u_i\rangle}{\partial t} + \rho\langle\partial_j u_i u_j\rangle = \langle\partial_j \mathrm{T}_{ij}\rangle. \tag{13}$$

Once again, we need to transform the inertial and the stress terms using equation (9) so that only the averages of the primitive flow variables are left in the final form instead of averages of their combinations or derivatives.

3.3.1 Inertial term. Following the approach of Gray (1975), we decompose the velocity as:

$$u_i = \langle u_i \rangle^f + u_i', \tag{14}$$

where $(\,)'$ represents local deviation from intrinsic averaged values. Applying equation (14) to the volume-averaged convective term:

$$\begin{aligned} \langle \partial_j u_i u_j \rangle &= \langle \partial_j (u_i' + \langle u_j \rangle^f)(u_j' + \langle u_j \rangle^f) \rangle \\ &= \langle \partial_j \langle u_i \rangle^f \langle u_j \rangle^f \rangle + \langle \partial_j u_i' u_j' \rangle + \langle \partial_j \langle u_i \rangle^f u_j' \rangle + \langle \partial_j \langle u_j \rangle^f u_i' \rangle. \end{aligned} \tag{15}$$

Using equation (9):

$$\langle \partial_j u_i u_j \rangle = \partial_j \langle \langle u_i \rangle^f \langle u_j \rangle^f \rangle + \frac{1}{V} \int_{A_{sf}} \langle u_i \rangle^f \langle u_j \rangle^f n_j \mathrm{dA} + \langle \partial_j u_i' u_j' \rangle + \langle \partial_j \langle u_i \rangle^f u_j' \rangle + \langle \partial_j \langle u_j \rangle^f u_i' \rangle. \tag{16}$$

Third and fourth terms can also be treated similarly:

$$\langle \partial_j \langle u_i \rangle^f u_j' \rangle = \partial_j \langle \langle u_i \rangle^f u_j' \rangle + \frac{1}{V} \int_{A_{sf}} \langle u_i \rangle^f u_j' n_j \mathrm{dA}. \tag{17}$$

Noting that $\langle u_j' \rangle = 0$ and $u_j' = u_j - \langle u_j \rangle^f$:

$$\langle \partial_j \langle u_i \rangle^f u_j' \rangle = \frac{1}{V} \int_{A_{sf}} \langle u_i \rangle^f u_j n_j \mathrm{dA} - \frac{1}{V} \int_{A_{sf}} \langle u_i \rangle^f \langle u_j \rangle^f n_j \mathrm{dA}. \tag{18}$$

Since the velocity is zero at the solid-fluid interface due to no-slip condition, the first integral term vanishes:

$$\langle \partial_j \langle u_j \rangle^f u_j' \rangle = -\frac{1}{V} \int_{A_{sf}} \langle u_i \rangle^f \langle u_j \rangle^f n_j \mathrm{dA}. \tag{19}$$

Thus, equation (16) becomes:

$$\langle \partial_j u_i u_j \rangle = \partial_j \langle \langle u_i \rangle^f \langle u_j \rangle^f \rangle - \frac{1}{V} \int_{A_{sf}} \langle u_i \rangle^f \langle u_j \rangle^f n_j \mathrm{dA} + \langle \partial_j u_i' u_j' \rangle. \tag{20}$$

For the first term on the right hand side of equation (20), note that $\langle u_i \rangle^f \langle u_j \rangle^f$ is a constant over the REV and average of the constant quantity is identical to itself. We choose to retain the integral term in equation (20) as it is not identically zero unless the pore geometry is symmetric.

The inertial term now becomes:

$$\langle \partial_j u_i u_j \rangle = \partial_j \langle u_i \rangle^f \langle u_j \rangle^f + \langle \partial_j u_i' u_j' \rangle - \frac{\langle u_i \rangle^f \langle u_j \rangle^f}{V} \int_{A_{sf}} n_j \mathrm{dA}. \tag{21}$$

Here, the second and the third terms on the right hand side cannot be evaluated with the sole knowledge of averaged flow quantities. These are two of the closure terms we will encounter in the final averaged form of the momentum equation. It is useful to note here that the integral term is identically zero for symmetric REV geometries.

3.3.2 Stress term. For a Newtonian fluid, the stress tensor can be written as:

$$T_{ij} = -p\delta_{ij} + \mu(\partial_i u_j + \partial_j u_i). \tag{22}$$

Averaging the stress term of the momentum equation by making use of the volume averaging theorem, i.e. Equation (9):

$$\langle \partial_j T_{ij} \rangle = -\partial_i \langle p \rangle + \mu \partial_j \langle \partial_i u_j + \partial_j u_i \rangle + \frac{1}{V} \int_{A_{sf}} T_{ij} n_j \mathrm{dA}. \tag{23}$$

For the second term on the right hand side, the volume averaging theorem needs to be applied once more:

$$\partial_j \langle \partial_i u_j + \partial_j u_i \rangle = \partial_j \partial_i \langle u_j \rangle + \partial_j^2 \langle u_i \rangle + \partial_j \left(\frac{1}{V} \int_{A_{sf}} (u_i n_i + u_j n_j) \mathrm{dA} \right). \tag{24}$$

For incompressible flows, $\partial_j \langle u_j \rangle = 0$ through the volume averaged continuity equation (equation (12)). Also note that the integral term is identically zero due to the fact that the fluid velocity is zero at the solid-fluid interface. Thus, the stress term becomes:

$$\langle \partial_j T_{ij} \rangle = -\partial_i \langle p \rangle + \mu \partial_j^2 \langle u_i \rangle + \frac{1}{V} \int_{A_{sf}} T_{ij} n_j \mathrm{dA}. \tag{25}$$

Using equations (13), (21) and (25), the averaged momentum equation becomes:

$$\begin{aligned} \rho \frac{\partial \langle u_i \rangle}{\partial t} + \frac{\rho}{\varepsilon^2} \partial_j \langle u_i \rangle \langle u_j \rangle = -\partial_i \langle p \rangle + \mu \partial_j^2 \langle u_i \rangle - \rho \langle \partial_j u_i' u_j' \rangle \frac{1}{V} \int_{A_{sf}} T_{ij} n_j \mathrm{dA} \\ + \frac{\rho \langle u_i \rangle^f \langle u_j \rangle^f}{V} \int_{A_{sf}} n_j \mathrm{dA}. \end{aligned} \tag{26}$$

All the terms of equation (26) except the last three on the right hand side are expressed in terms of averaged velocity components. So, the knowledge of the bulk fluid motion will suffice in evaluating them. However, the remaining three terms require a closure methodology.

3.4 Closure of momentum equation

Direct computation of equation (26) necessitates complete knowledge of fluid flow throughout the porous media. Most porous media applications require a high number of pores for effective cooling or filtering. Therefore, the direct computation approach is rarely feasible. Answer to this problem has conventionally been to link the closure terms in equation (26) to the Ergun relation (equation (4)) (Vafai and Tien, 1981) as:

$$\rho \frac{\partial \langle u_j \rangle}{\partial t} + \frac{\rho}{\varepsilon^2} \partial_j \langle u_i \rangle \langle u_j \rangle = -\partial_i \langle p \rangle + \mu \partial_j^2 \langle u_i \rangle - \frac{\mu}{K} \langle u_i \rangle - \frac{C_E}{\sqrt{K}} \rho |\langle u_i \rangle| \langle u_i \rangle. \tag{27}$$

While equation (4) only relates the bulk pressure drop to the total mass flow rate, the solution of equation (27) provides local volume averaged flow field information throughout the porous media. Equation (27) is very similar in form to the Navier-Stokes equations. This enables easy handling of conjugate open flow (without porous media)

and porous flow problems and permits application of no-slip conditions at the solid walls bounding the solid matrix. By this treatment, the problem is reduced to determination of two parameters, namely, permeability, K and Ergun coefficient, C_E. Note that there is no fundamental reason for equation (27) to be correct. Both experimental and heuristic methods of estimating the permeability and the Ergun coefficient use the Darcy's law (equation (1)) or Ergun relation (equation (4)) as basis, making the rest of the terms in equation (27) stand out as error terms. However, in most tightly packed porous media, momentum loss is largely due to the pore scale flow structures. In these cases, porous source terms are dominant over the other terms in the averaged momentum equation. Thus, generally, equation (27) is expected to closely follow equation (4).

In closing the local volume averaged momentum equation, Whitaker (1996) develops a more rigorous method. With the help of a series of scaling arguments, he derives governing equations for the velocity and pressure deviations from the local averaged value. He then develops boundary value problems for permeability and Forchheimer tensors to be solved over a representative, periodic unit-cell of the porous media geometry.

In our multi-scale method, we take a similar but more basic route and directly compute the closure terms appearing in local volume averaged momentum equation (equation (26)). We take advantage of the fact that most porous media consist of a matrix of repeating pore patterns. So, instead of computing the flow field in each pore, we try to get away with modeling a single one of each repeating pore patterns observed in a given porous media. The closure terms for each pore model can then be computed for a range of flow speeds, allowing us to construct the closure terms accurately as functions of position and flow speed:

$$\rho\frac{\partial\langle u_i\rangle}{\partial t}+\frac{\rho}{\varepsilon^2}\partial_j\langle u_i\rangle\langle u_j\rangle=-\partial_i\langle p\rangle+\mu\partial_j^2\langle u_i\rangle+S(x_j,u_j). \tag{28}$$

Where $S(x_j, u_j)$ is the closure functional established via the multi-scale method. Note that the closure functional acts as a source term in the local volume averaged momentum equation. Thus, existing Navier-Stokes solvers can be used to compute this kind of problems with very little modification for the porous zones. Computational cost associated with this multi-scale approach strongly depends on the level of uniformity and complexity of the pores. For a uniform porous media, only one pore model is needed. In our method, we do not need to refer to the concepts of permeability and the Ergun coefficient. Nonetheless, we can easily derive the expressions for these by comparing equations (26) and (27):

$$K=-\mu\langle u_i\rangle\left[\frac{1}{V}\int_{A_{sf}}T_{ij}n_j\mathrm{dA}\right]^{-1}, \tag{29}$$

$$C_E=\frac{\sqrt{K}}{|\langle u_i\rangle|\langle u_i\rangle}\left[\langle\partial_j u_i'u_j'\rangle-\frac{\langle u_i\rangle^f\langle u_j\rangle^f}{V}\int_{A_{sf}}n_j\mathrm{dA}\right]. \tag{30}$$

3.5 Averaging of the energy equation

Consider the fluid phase energy equation with constant specific heat and no heat sources:

$$(\rho c_p)_f \left(\frac{\partial T_f}{\partial t} + \partial_i u_i T_f \right) = k_f \partial_j^2 T_f. \tag{31}$$

Applying local volume averaging:

$$(\rho c_p)_f \left(\frac{\partial \langle T_f \rangle}{\partial t} + \langle \partial_i u_i T_f \rangle \right) = k_f \langle \partial_j \partial_j T_f \rangle. \tag{32}$$

Using equation (9), the diffusive term can be expanded as:

$$\begin{aligned} k_f \langle \partial_j \partial_j T_f \rangle &= k_f \partial_j \langle \partial_j T_f \rangle + \frac{k_f}{V} \int_{A_{sf}} n_j \partial_j T_f \mathrm{dA} \\ &= k_f \partial_j^2 \langle T_f \rangle + \frac{k_f}{V} \partial_j \int_{A_{sf}} n_j T_f \mathrm{dA} + \frac{k_f}{V} \int_{A_{sf}} n_j \partial_j T_f \mathrm{dA}. \end{aligned} \tag{33}$$

Defining a local temperature deviation as:

$$T_f = \langle T_f \rangle^f + T_f', \tag{34}$$

and employing the divergence theorem, the first integral term in equation (33) becomes:

$$\int_{A_{sf}} n_j T_f \mathrm{dA} = \int_{A_{sf}} n_j \langle T_f \rangle^f \mathrm{dA} + \int_{A_{sf}} n_j T_f' \mathrm{dA} = \int_V \partial_j \langle T_f \rangle^f \mathrm{dV} + \int_{A_{sf}} n_j T_f' \mathrm{dA}. \tag{35}$$

Noting that the variation of an averaged quantity within the averaging volume itself is zero, the first integral vanishes. We then arrive at the averaged diffusion term:

$$k_f \langle \partial_j \partial_j T_f \rangle = k_f \partial_j^2 \langle T_f \rangle + \frac{k_f}{V} \partial_j \int_{A_{sf}} n_j T_f' \mathrm{dA} + \frac{k_f}{V} \int_{A_{sf}} n_j \partial_j T_f \mathrm{dA}. \tag{36}$$

Averaging of the convection term yields:

$$\langle \partial_i u_i T_f \rangle = \partial_i \langle u_i T_f \rangle + \frac{1}{V} \int_{A_{sf}} u_i T_f n_i \mathrm{dA}. \tag{37}$$

The integral term on the right hand side of equation (37) vanishes due to no-slip condition at the solid-fluid walls. Using equation (34), we decompose the convection term as:

$$\begin{aligned} \langle \partial_i u_i T_f \rangle &= \partial_i \langle (\langle u_i \rangle^f + u_i')(\langle T_f \rangle^f + T_f') \rangle \\ &= \partial_i \langle \langle u_i \rangle^f \langle T_f \rangle^f + \langle u_i \rangle^f T_f' + u_i' \langle T_f \rangle^f + u_i' T_f' \rangle. \end{aligned} \tag{38}$$

Knowing that $\langle \psi' \rangle$, the volume-averaged convection term is obtained:

$$\langle \partial_i u_i T_f \rangle = \partial_i \langle u_i \rangle^f \langle T_f \rangle^f + \varepsilon \partial_i \langle u_i' T_f' \rangle^f. \tag{39}$$

Substituting equations (39) and (36) in equation (32), we obtain the volume-averaged energy equation for the fluid phase:

$$\varepsilon(\rho c_p)_f\left(\frac{\partial\langle T_f\rangle^f}{\partial t}+\frac{1}{\varepsilon}\partial_i\langle u_i\rangle^f\langle T_f\rangle^f+\partial_i\langle u_i'T_f'\rangle^f\right)$$
$$=\varepsilon k_f\partial_j^2\langle T_f\rangle^f+\frac{k_f}{V}\partial_j\int_{A_{sf}}n_jT_f'\mathrm{dA}+\frac{k_f}{V}\int_{A_{sf}}n_j\partial_jT_f\mathrm{dA}. \tag{40}$$

Similarly, for the solid phase, the volume-averaged energy equation is:

$$(1-\varepsilon)(\rho c_p)_s\frac{\partial\langle T_s\rangle^s}{\partial t}=(1-\varepsilon)k_s\partial_j^2\langle T_s\rangle^{\mathrm{s}}+\frac{k_s}{V}\partial_j\int_{A_{fs}}n_jT_s'\mathrm{dA}+\frac{k_s}{V}\int_{A_{\mathrm{fs}}}n_j\partial_jT_s\mathrm{dA}. \tag{41}$$

In many practical problems, the temperature difference between the solid and fluid phases inside an REV is much smaller than the global scale temperature variation. This condition is met if the REV is much smaller compared to global length scale, there is no heat generation or loss inside the REV and temperature distribution does not vary or vary slowly over time. Under these conditions, we can assume "local thermodynamic equilibrium" which grants:

$$\langle T_f\rangle^f=\langle T_s\rangle^s=\langle T\rangle. \tag{42}$$

At the solid-fluid interface, the following boundary conditions apply:

$$T_f'\big|_{A_{sf}}=T_s'\big|_{A_{sf}}, \tag{43}$$

$$k_f\partial_jT_f\big|_{A_{sf}}=k_s\partial_jT_s\big|_{A_{sf}}. \tag{44}$$

Also noting that $\mathbf{n}_{sf}=-\mathbf{n}_{fs}$, and adding equations (40) and (41), we obtain the local volume averaged energy equation:

$$\left[\varepsilon(\rho c_p)_f+(1-\varepsilon)(\rho c_p)_s\right]\frac{\partial\langle T\rangle}{\partial t}+\frac{1}{\varepsilon}(\rho c_p)_f\partial_i\langle u_i\rangle\langle T\rangle$$
$$=\left[\varepsilon k_f+(1-\varepsilon)k_s\right]\partial_j^2\langle T\rangle+\frac{k_f-k_s}{V}\partial_j\int_{A_{sf}}n_jT_f'\mathrm{dA}-\varepsilon(\rho c_p)_f\partial_i\langle u_i'T_f'\rangle^f. \tag{45}$$

Equation (45) introduces two additional closure terms for non-isothermal problems. Nozad *et al.* (1985) derive governing equations for T_f' and T_s' and introduce constitutive relationships between these temperature deviations and local volume averaged temperature gradient via transformation vectors such as:

$$T_f'=f_i\partial_i\langle T\rangle+\psi\quad T_s'=g_i\partial_i\langle T\rangle+\xi. \tag{46}$$

He then develops boundary value problems for f_i and g_i to be solved over a representative unit-cell.

Amiri and Vafai (1994) treat the closure terms in equation (45) as an interfacial heat transfer term between fluid and the solid phases. They use empirical correlations for the specific surface area and heat transfer coefficient to close the energy equation.

We handle the energy closure terms the same way as the momentum equation counterparts with the multi-scale method. The last two terms on the right hand side

of equation (45) can be computed over the chosen sample pore models for a range of temperature values. Thus, we can avoid any constitutive or empirical relations by taking a direct approach.

In the current work, we will focus on an isothermal problem. However, we presented the derivation of the local volume averaged energy equation for completeness and as a step towards our goal of simulating the transpiration cooling of the liquid rocket engine injector face plate.

4. Numerical method and assessment of the present porous media model

We have shown that the local volume averaged continuity equation is unchanged and momentum equation is very similar in form to the regular Navier-Stokes equations with additional momentum source terms and the convection term modified by a factor of porosity squared, ε^2. Thus, a Navier-Stokes solver can easily be modified to account for porous media.

The proposed formulation has been implemented in Navier-Stokes solvers (Thakur *et al.*, 2002; Kamakoti *et al.*, 2006). Porous zones are designated by coordinate ranges and the previously calculated source terms are added to the momentum equation components.

4.1 Isothermal flow through a drilled orifice plate

This test case consists of a porous plate placed in a cylindrical channel as shown in Figure 5. The porous material used herein is a metallic plate with an array of uniform and evenly distributed drilled holes. Owing to its simple and well defined pore geometry, this case is attractive for testing the multi-scale method developed here. The hole pattern details are shown in Figure 6.

This problem was studied before by Tully *et al.* (2005) both numerically and experimentally. The porous plate was inserted in a cylindrical channel test section and pressure drop values were recorded for a range of average flow speeds as summarized in Table I.

4.1.1 Pore model. The porous metallic plate has a uniform array of circular through holes distributed along its surface. Therefore, the pore shape is simply a circular tube.

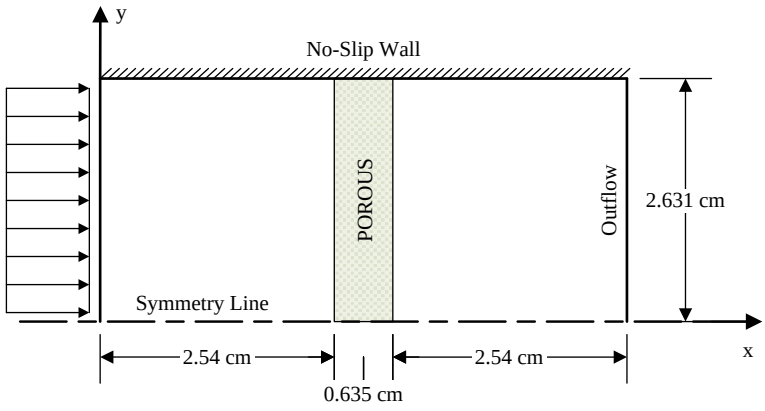

Figure 5.
Problem domain

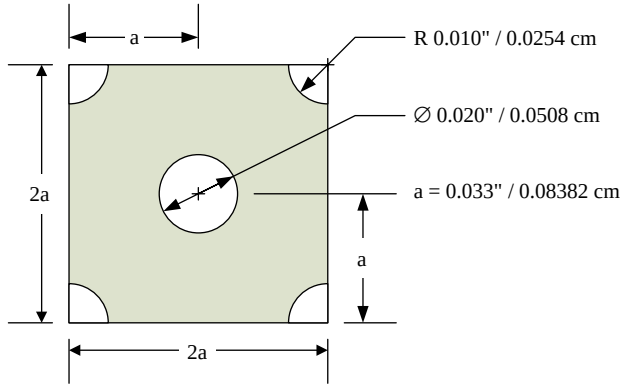

Figure 6.
Hole pattern details

Fluid properties (air @ 24.2 °C)		Inlet filter velocities (m/s)	
Density (ρ)	1.1875 kg/m^3	U_{D1}	13.1
Dynamic viscosity (μ)	1.8048×10^{-5} kg/m s	U_{D2}	16.3
Specific heat (c_p)	1,006.2 J/kg K	U_{D3}	18.1
Thermal conductivity (k)	0.025913 W/m K	U_{D4}	20.1
		U_{D5}	23.3
		U_{D6}	25.8

Table I.
Summary of experimental conditions

In order to account for the momentum loss as the flow adjusts to enter the pores, we extend the pore domain for three hole diameters towards upstream direction.

Isothermal fluid flow through the pore is computed for the range of flow speeds listed in Table I. Equations (29) and (30) are evaluated to find the permeability and Ergun coefficient for each flow speed in conjunction with equation (27) for the global domain. Results of the pore-scale analysis are listed in Table II which clearly shows that in contrast to conventional assumption, permeability and the Ergun coefficient vary significantly with changing flow speeds and are not material properties.

4.1.2 Global domain. With the closure parameters obtained via the pore-scale analysis, flow through the global domain as shown in Figure 5 is computed. In the porous zone, Navier-Stokes equations are replaced with equation (27). Pressure drop values across the centerline are plotted in comparison to the experimental results by Tully *et al.* (2005) in Figure 7.

U_D (m/s)	Re_D	K (m^{-2})	C_E
13.1	438	2.29×10^{-10}	1.38×10^{-2}
16.3	545	1.92×10^{-10}	1.26×10^{-2}
18.1	605	1.76×10^{-10}	1.21×10^{-2}
20.1	672	1.61×10^{-10}	1.15×10^{-2}
23.3	779	1.43×10^{-10}	1.08×10^{-2}
25.8	862	1.30×10^{-10}	1.03×10^{-2}

Table II.
Pore-scale analysis results

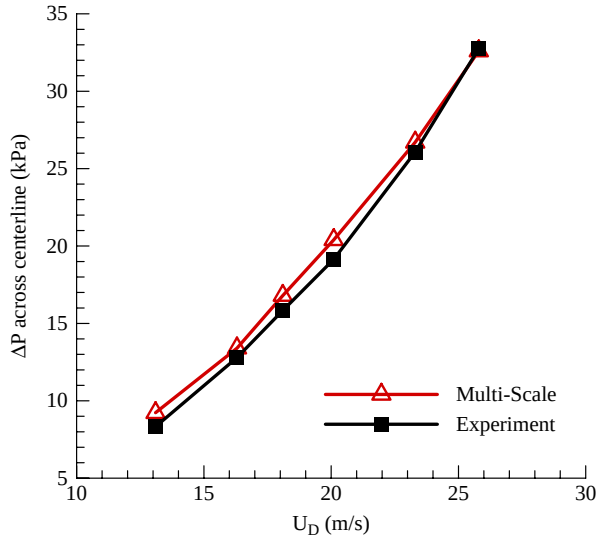

Figure 7.
Pressure drop across centerline v. filter velocity

Figure 7 shows that the experimental data are closely reproduced by the multi-scale method. The error relative to the experimental data ranges between 11 and 1 percent for the lowest and highest flow speeds, respectively.

5. Summary and conclusion

A first principle based, multi-scale method is developed for numerical simulations of fluid flow through porous media. In the present model, the effect of porous structures on the global fluid flow is accounted for via local volume averaged governing equations, while the closure terms are accounted for via averaging flow characteristics around the pores. Hence, empirical dependence of simulations is removed without requiring excessive computational cost. The performance of the model has been tested for an isothermal flow case. Both the permeability and Ergun coefficient are shown to be flow properties as opposed to the empirical approach which typically results in constant values of these parameters independent of the flow conditions. Hence, the present multi-scale approach is more versatile and can account for the possible changes in flow characteristics.

References

Amiri, A. and Vafai, K. (1994), "Analysis of dispersion effects and non-thermal equilibrium, non-Darcian, variable porosity incompressible flow through porous media", *International Journal of Heat and Mass Transfer*, Vol. 37 No. 6, pp. 939-54.

Beavers, G.S. and Joseph, D.D. (1967), "Boundary conditions at a naturally permeable wall", *The Journal of Fluid Mechanics*, Vol. 30, pp. 197-207.

Bejan, A. and Poulikakos, D. (1984), "The non-Darcy regime for vertical boundary layer natural convection in a porous medium", *International Journal of Heat and Mass Transfer*, Vol. 27, pp. 717-22.

Brinkman, H.C. (1947), "A calculation of the viscous force exerted by a flowing fluid on a dense swarm of particles", *Applied Scientific Research*, Vol. A1, pp. 27-34.

Brinkman, H.C. (1948), "On the permeability of media consisting of closely packed porous particles", *Applied Scientific Research*, Vol. A1, pp. 81-6.

Carman, P.C. (1937), "The determination of the specific surface area of powder I", *Journal of the Society of Chemical Industry*, Vol. 57, pp. 225-34.

Cheng, P. (1977), "Combined free and forced boundary layer flows about inclined surfaces in a porous medium", *International Journal of Heat and Mass Transfer*, Vol. 20, pp. 807-14.

Cheng, P. and Minkowycz, W.J. (1977), "Free convection about a vertical flat plate embedded in a porous medium with application to heat transfer from a Dyke", *Journal of Geophysical Research*, Vol. 82, pp. 2040-4.

Darcy, H. (1856), *Les Fontaines Publiques de la ville de Dijon*, Dalmont, Paris.

Dullien, F.A.L. (1979), *Porous Media: Fluid Transport and Pore Structure*, Academic Press, New York, NY.

Ergun, S. (1952), "Fluid flow through packed column", *Chemical Engineering Progress*, Vol. 48, pp. 89-94.

Forchheimer, P. (1901), "Wasserbewegung durch Boden", *Z Ver Deutsch Ing*, Vol. 45, pp. 1782-8.

Gray, W.G. (1975), "A derivation of the equations for multiphase transport", *Chemical Engineering Science*, Vol. 30, pp. 229-33.

Happel, J. and Brenner, H. (1986), *Low Reynolds Number Hydrodynamics*, Martinus Nijhoff Publishers, Dordrecht.

Kamakoti, R., Thakur, S., Wright, J. and Shyy, W. (2006), "Validation of a new parallel all-speed CFD code in a rule-based framework for multidisciplinary applications", paper presented at 36th AIAA Fluid Dynamics Conference and Exhibit, AIAA, Paper No. 2006-3063.

Kaviany, M. (1991), *Principles of Heat Transfer in Porous Media*, Springer-Verlag, New York, NY.

Lin, G. and Hu, J. (2007), private communication, Department of Mechanical Engineering, University of Michigan, Ann Arbor, MI.

Liu, J.Y., Minkowycz, W.J. and Cheng, P. (1986), "Conjugated, mixed convection-conduction heat transfer along a cylindrical fin in a porous medium", *International Journal of Heat and Mass Transfer*, Vol. 29, pp. 769-75.

Lundgren, T.S. (1972), "Slow flow through stationary random beds and suspension of spheres", *The Journal of Fluid Mechanics*, Vol. 51, pp. 273-99.

Macdonald, I.F., El-Sayed, M.S., Mow, K. and Dullien, F.A.L. (1979), "Flow through porous media – Ergun equation revisited", *Industrial and Engineering Chemistry Fundamentals*, Vol. 18, pp. 199-208.

Nield, D.A. and Bejan, A. (1992), *Convection in Porous Media*, Springer-Verlag, New York, NY.

Nozad, I., Carbonell, R.G. and Whitaker, S. (1985), "Heat conduction in multi-phase systems I: theory and experiments for two-phase systems", *Chemical Engineering Science*, Vol. 40, pp. 843-55.

Rubinstein, J. (1982), "Effective equations for flow in random porous media with a large number of scales", *The Journal of Fluid Mechanics*, Vol. 170, pp. 379-83.

Shyy, W. (1994), *Computational Modeling for Fluid Flow and Interfacial Transport*, Elsevier, Amsterdam.

Slattery, J.C. (1969), "Single-phase flow through porous media", *AIChE Journal*, Vol. 15, pp. 866-72.

Slattery, J.C. (1981), *Momentum, Energy and Mass Transfer in Continua*, 2nd ed., R.F. Krieger Publishing, Huntington, NY.

Sparrow, E.M. and Loeffler, A.L. Jr (1959), "Longitudinal laminar flow between cylinders arranged in regular array", *AIChE Journal*, Vol. 5, pp. 328-30.

Sutton, G.P. (2003), "History of liquid propellant rocket engines in the United States", *Journal of Propulsion and Power*, Vol. 19 No. 6, pp. 978-1007.

Thakur, S., Wright, J. and Shyy, W. (2002), "Stream: a computational fluid dynamics and heat transfer Navier-Stokes solver. Theory and applications", Streamline Numerics, Inc. and Computational Thermo-Fluids Laboratory, Department of Mechanical and Aerospace Engineering Technical Report, Gainesville, FL.

Tully, L.R., Omar, A., Chung, J.N. and Carroll, B.F. (2005), "Fluid flow and heat transfer in a liquid rocket fuel injector", paper presented at AIAA/ASME/SAE/ASEE Joint Propulsion Conference & Exhibit, AIAA-2005-4127.

Vafai, K. and Tien, C-L. (1981), "Boundary and inertia effects on flow and heat transfer in porous media", *International Journal of Heat and Mass Transfer*, Vol. 24, pp. 195-203.

Ward, J.C. (1964), "Turbulent flow in porous media", *Journal of Hydraulic Division ASCE*, Vol. HY5, pp. 1-12.

Whitaker, S. (1969), "Advances in theory of fluid motion in porous media", *Ind. Eng. Chem.*, Vol. 61, pp. 14-28.

Whitaker, S. (1996), "The Forchheimer equation: a theoretical development", *Transport in Porous Media*, Vol. 25, pp. 27-61.

Corresponding author
Emre Sozer can be contacted at: esozer@umich.edu